Quantum Information and Computation, Vol. 0, No. 0 (2003) 000–000
© Rinton Press

arXiv:1612.07593v2 [quant-ph] 26 Dec 2016

Robustness of quantum neural calculation increases with system size

Nam H. Nguyen and Elizabeth C. Behrman [a]
Department of Mathematics and Physics, Wichita State University
Wichita, KS 67260-0033, USA

James E. Steck
Department of Aerospace Engineering, Wichita State University
Wichita, KS 67260-0044, USA

Received (received date)
Revised (revised date)

In previous work, we have shown that quantum neural computation is robust to noise and decoherence for a two-qubit system. Here we extend our results to three-, four-, and five-qubit systems, and show that the robustness to noise and decoherence is maintained and even improved as the size of the system is increased.

Keywords: quantum computing, entanglement, dynamic learning, noise, decoherence, bootstrap
Communicated by: to be filled by the Editorial

1 Introduction

Quantum computing remains a bright hope for classically difficult calculations [1], and, more fundamentally, for understanding the nature of reality [2]. But major problems remain in scaling up from 'proof of concept' hardware to the sizes that will be necessary to do the interesting problems. Among the most recalcitrant are the problems of noise [3] and decoherence [4].

Classically, noise can be dealt with using the theory of stochastic processes[5]. Some previous authors have proposed dealing with noise in quantum computers by using ancilla [6, 7]. The problem with this approach is that the number of ancilla necessary grows very rapidly, and, scaleup is already a difficulty. Decoherence is a uniquely quantum problem: with coherence lost, the computation loses its quantum nature (and, thus, the whole point of our doing it in the first place.)

Some recent papers on these problems are those of Glickman [8], Takahashi [9], Roszak [10], Dong[11], and Cross[12]. Glickman et al. used the scattering of photons to better understand the process of decoherence. Their experience shows that it might be possible to control decoherence in a quantum system by taking advantage of an atom's spin state. Takahashi et al. were able to use high magnetic fields to suppress quantum decoherence to levels far below the threshold necessary for quantum information processing. Roszak et al.

[a]Corresponding author
Email address: behrman@math.wichita.edu

proposed a general approach to protect a two level system against decoherence by engineering a non-classical multiple superposition of coherent states in a non-Markovian reservoir. Dong et al.[11] presented a systematic numerical methodology called sampling-based control for robust quantum design of a quantum systems. This method is similar to ours in that it also uses machine learning. In the training step, the control is learned using a gradient flow based learning algorithm for an augmented system constructed from samples. Cross et al. [12] showed that quantum learning is robust to noise by showing that the complexity of learning between classical and quantum method is the same. However, when noise is being introduced, the best classical algorithm will have superpolynomial complexity, whereas, the complexity in quantum algorithms is only logarithmic.

In our own work, we have shown that for a two qubit system, a quantum neural network (QNN) approach to entanglement calculation is robust to the introduction of both noise and decoherence [13]. Here we generalize to a larger system and show that in fact the robustness improves with size.

2 Dynamic learning for the quantum system

We begin with the general form of the Schrodinger equation:

$$\frac{d\rho}{dt} = \frac{1}{i\hbar}[H, \rho] \tag{1}$$

where ρ is the density matrix and H is the Hamiltonian. For an N-qubit system, we define the Hamiltonian to be

$$H = \sum_{\alpha=1}^{N} K_\alpha \sigma_{x\alpha} + \epsilon_\alpha \sigma_{x\alpha} + \sum_{\alpha=1}^{N} \zeta_{\alpha\beta} \sigma_{z\alpha} \sigma_{z\beta} \tag{2}$$

where $\{\sigma\}$ are the Pauli operators corresponding for each qubit, $\{K\}$ are the tunneling amplitudes for each qubit tunnel between states, $\{\epsilon\}$ are the biases, and $\{\zeta\}$ are the qubit-qubit couplings. We choose the usual charge basis, in which each qubit's state is 0 or 1.

By introducing the Liouville operator, $L = \frac{1}{i\hbar}\big[\cdots, H\big]$, equation (1) can be rewritten as

$$\frac{\partial\rho}{\partial t} = -iL\rho \tag{3}$$

which has the general solution of

$$\rho(t) = e^{-iLt}\rho(0) \tag{4}$$

Notice that the time evolution of the system is directed by the parameters $\{K, \epsilon, \zeta\}$. That is, if one or more of them is changed, the way a given state evolves in time will also change. Thus, equation (4) is mathematically isomorphic to the equation for information propagation in a neural network:

$$\phi_i = \sum_j \omega_{ij} f_j(\phi_i) \qquad \phi_{output} = F_W \phi_{input} \tag{5}$$

where ϕ_{output} is the output vector of the network, ϕ_{input} is the input vector, and F_W is the network operator, which depends on the neuron connectivity weight matrix W. Note that

$W \in C^n$ since our network takes on complex valued weights. Classically complex valued networks have been shown to be more powerful than real valued networks. For instance, a complex valued neural network can solve the nonlinear XOR problem without a hidden layer[14].

In our quantum neural computer, the role of the input vector is played by the initial density matrix $\rho(0)$, the role of the output is played by the density matrix at the final time, $\rho(t_f)$, and $\{K, \epsilon, \zeta\}$ play the role of the weights of the network. We then can train the system to evolve in time to a set of a particular final states at the final time t_f by adjusting the parameters $\{K, \epsilon, \zeta\}$ through a gradient descent learning algorithm. Time evolution is a quantum mechanical property; hence, a quantum mechanical function, such as an entanglement witness of the initial state, can be mapped to an observable (a measure) of the system's final state. The detailed derivation and analysis of our learning algorithm for the QNN can be found in [15].

3 Learning with perturbation to the density matrix

In previous work, we have shown that quantum neural computation is robust under random perturbations of the density matrix for the two qubit quantum system [13]. We now generalize this result by extending our previous work to three, four and five qubit quantum systems and show that the increase in the number of qubits improves robustness to both 'noise' and 'decoherence.' Note that we define 'noise' as perturbation to the magnitude of the elements of the density matrix, while 'decoherence' is the perturbation to the phase. Splitting the density matrix this way is possible since we are working with numerical simulation. Of course, the density matrix must remain Hermitian, positive definite, and with unit trace to conserve probability.

As we did with the two-qubit system, we will investigate the effects of noise during training and during testing. Further, we can use knowledge of the smaller system as 'partial knowledge' of the larger system, in finding the set of parameter functions that will perform the desired computation. We call this 'bootstrapping'[16]. In previous work[17] we successfully used this technique to find an entanglement indicator for a general multiqubit system. In that work, we trained the two-qubit system to output an entanglement indicator, then used those functions as the starting point for training the three-qubit system. From three we bootstrapped to four, and so on, and in each case, the amount of additional training necessary decreased, because more and more of the information necessary for the entanglement indicator was present already in the N-1 qubit system.

3.1 Three qubit system

For a three qubit system, our Hamiltonian is

$$H = K_A\sigma_{xA}+K_B\sigma_{xB}+K_C\sigma_{xC}+\epsilon_A\sigma_{zA}+\epsilon_B\sigma_{zB}+\zeta_{AB}\sigma_{zA}\sigma_{zB}+\zeta_{AC}\sigma_{zA}\sigma_{zC}+\zeta_{BC}\sigma_{zB}\sigma_{zC} \quad (6)$$

The increased connectivity is evident in the increased number of qubit-qubit terms: While with the two-qubit system there is but one, with the three-qubit system there are three. Since we are training for a symmetric measure, the tunneling functions $K_A = K_B = K_C$, and similarly for the ϵ and ζ functions. We now have more measures that need to be trained, however: we need to be able to distinguish among entanglement between qubits A and B,

between A and C, between B and C, and among A, B, and C (three-way entanglement; see [17] for details.) Thus, the number of training pairs, and therefore the amount of possible training, goes up like the connectivity; were it not for bootstrapping, this would indeed be a daunting challenge.

For the two-qubit system, we used a training set of four [15]; thus, for the three-qubit system, we need a set of thirteen: three sets of four for the three pairwise entanglements, and one more for three-way entanglement. Table 1 shows our training data when there is no noise added to the system.

Table 1. The four training pairs for the pairwise QNN entanglement witness. For the 3-qubit system, this set of four was used for each of the three pairs of qubits, outerproducted with the state $|0\rangle$ for the third; the thirteenth training pair was the three-way entangled state $|000\rangle + |111\rangle$. States are given in the Table without their normalizing factor for clarity.

Input state	Target	Trained
Bell $= |00\rangle + |11\rangle$	1.0	0.998
Flat $= |00\rangle + |01\rangle + |10\rangle + |11\rangle$	0.0	1.3×10^{-5}
$C = 0.5|10\rangle + |11\rangle$	0.0	1.9×10^{-4}
$P = |00\rangle + |10\rangle + |11\rangle$	0.44	0.44
RMS	1.8×10^{-3}	
Epochs	30	

The parameter functions $\{K, \epsilon, \zeta\}$ have similar characteristics to the two qubit system parameter functions. Once these parameters functions are trained, we can use them to test other states. The results on these testing states, which can be either pure or mixed, tell us whether the system has correctly generalized (learned). We found that all three functions are easily parametrized as simple oscillating functions. Figures 1-3 show the actual trained parameters in dashed lines and their Fourier fit in solid lines.

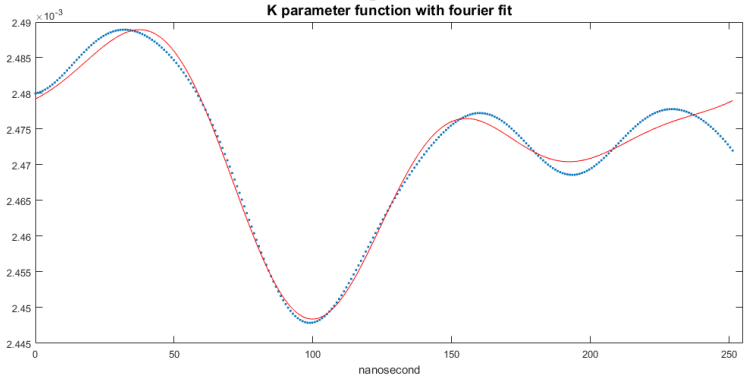

Fig. 1. K parameter function trained with zero noise or decoherence, for the 3-qubit system.

Testing using the Fourier fit parameter functions give identical (within computational error) results as testing with the trained parameter pointwise data; i.e, the differences between the data points and the fits are small enough not to matter. Table 2 shows the fitted param-

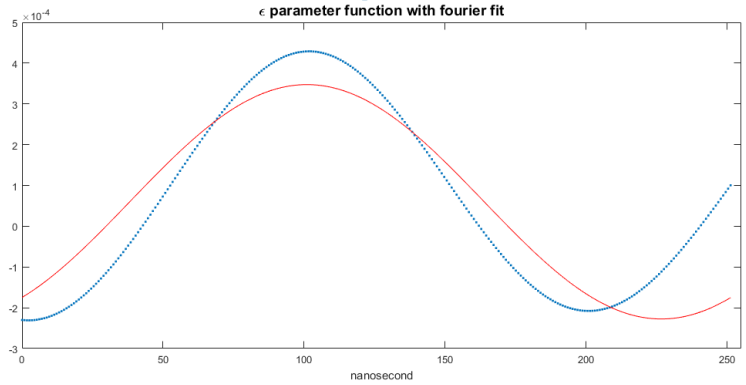

Fig. 2. ϵ parameter function trained with zero noise or decoherence, for the 3-qubit system.

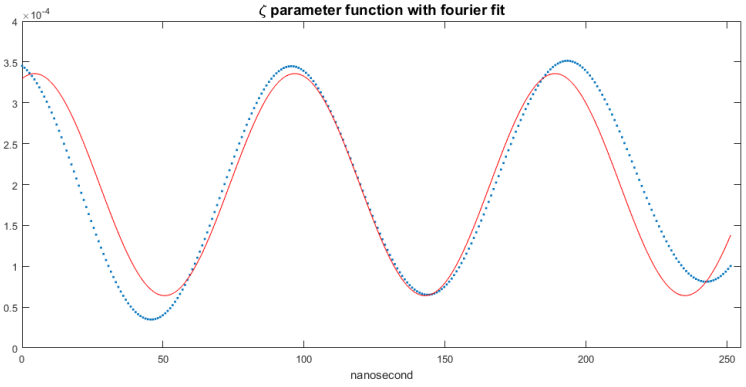

Fig. 3. ζ parameter function trained with no noise or decoherence, for the 3-qubit system.

eter functions' Fourier coefficients for zero noise.

Table 2. Fourier coefficients for 3-qubit fitted parameter functions with no noise and decoherence.

Coefficients	K	ϵ	ζ
a_0	0.002472	5.993×10^{-5}	1.999×10^{-4}
a_1	1.071×10^{-6}	-2.345×10^{-4}	1.297×10^{-4}
b_1	-1.103×10^{-6}	1.661×10^{-4}	4.043×10^{-5}
a_2	-1.109×10^{-6}	——	——
b_2	1.023×10^{-7}	——	——
ω	0.02498	0.02498	0.05750
RMS	9.774×10^{-7}	1.840×10^{-6}	7.291×10^{-6}

$$f(t) = a_0 + a_1 \cos(\omega t) + b_1 \sin(\omega t) + a_2 \cos(\omega t) + b_2 \sin(\omega t)$$

We then proceed by adding noise and decoherence to the system. To do this, we first trained the 2-qubit sytem with no noise or decoherence, then bootstrap[16] the already trained parameter functions $\{K, \epsilon, \zeta\}$ to the three qubit system. We have found that this helped to decrease the number of epochs needed to train the system [17]. We steadily increased the perturbation to the density matrix and found that the 3-qubit system parameters are more stable to noise and decoherence than the 2-qubit system. That is, the data points on the parameter functions deviate less as noise, decoherence, or both, are added. Results of the parameter functions for the 3-qubit system, trained at 0.0089 phase noise (decoherence), are shown in Figures 4-6. The level of noise we report is the amplitude, that is, the root-mean-square-average size of these random numbers, imposed at each timestep.

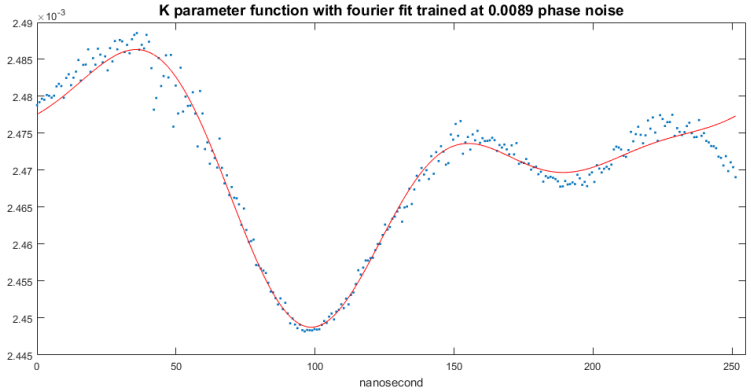

Fig. 4. Parameter function K trained at 0.0089 amount of decoherence in a 3-qubit system. The solid red curve represents the Fourier fit of the actual data points.

At equal amounts of phase noise added to the density matrix, the data points for the three-qubit system are less scattered than the parameter functions for the two qubit system. Magnitude noise gives similar results. We can of course add both noise and decoherence to

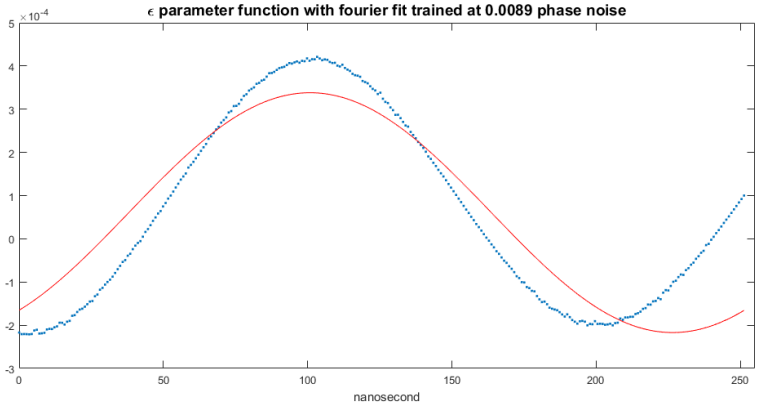

Fig. 5. Parameter function ϵ trained at 0.0089 decoherence in a 3-qubit system. The solid red curve represents the Fourier fit of the actual data points.

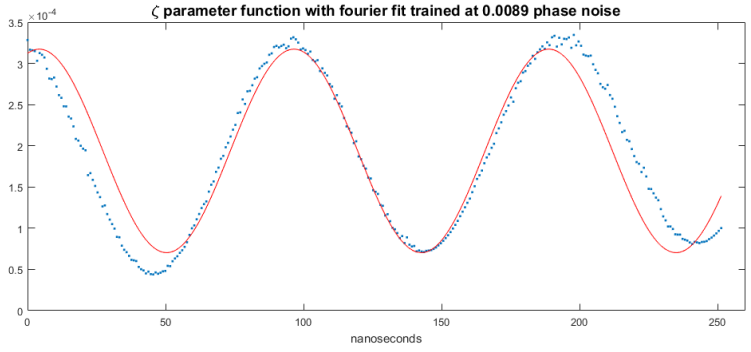

Fig. 6. Parameter function ζ trained at 0.0089 decoherence in a 3-qubit system. The solid red curve represents the Fourier fit of the actual data points.

the system simultaneously (we called this 'total noise'.) As with the two-qubit system in our earlier work [13], we graph the Fourier coefficients of each parameter function as a function of total noise. Figures 7-9 show that the coefficients, and therefore the parameter functions, change very little.

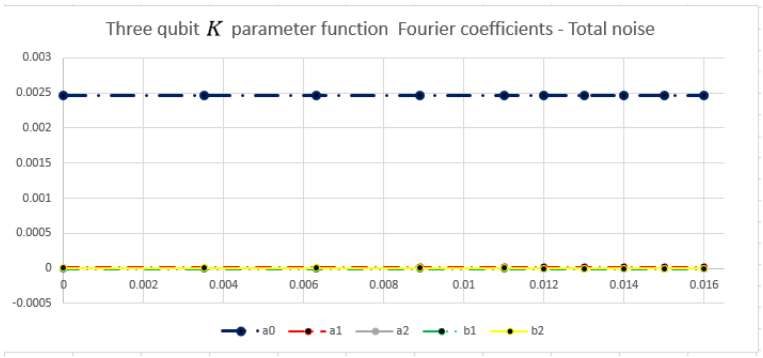

Fig. 7. Parameter function K Fourier coefficients as a function of total noise for the 3-qubit system. Lines are drawn to guide the eye.

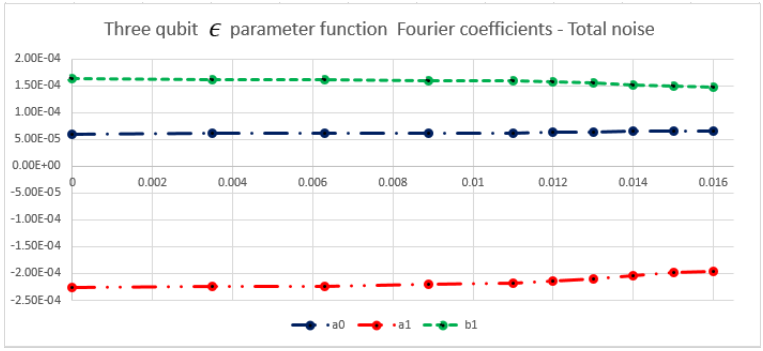

Fig. 8. Parameter function ϵ Fourier coefficients as a function of total noise for the 3-qubit system. Lines are drawn to guide the eye.

Thus far we have shown that our system is robust to noise and decoherence during the learning process. We need also to test these learned parameters on some 'testing' states (i.e., not in the training set) to see how well the system has actually learned, and what the effect of the noise is on the performance. We chose a pure state P and a mixed state M for this process. We choose P to be

$$P = |1\ \gamma\ 0\ 1\ 0\ 0\ 0\ 0\rangle \otimes \langle 1\ \gamma\ 0\ 1\ 0\ 0\ 0\ 0| \quad \text{for} \quad 0 \leq \gamma \leq 1$$

which is pairwise entangled between qubits B and C, as a function of γ. Figure 11 shows the testing of this state, as a function of γ, for increasing amounts of (total) noise. There is some spread but the behavior is qualitatively correct, and the indicator relatively stable.

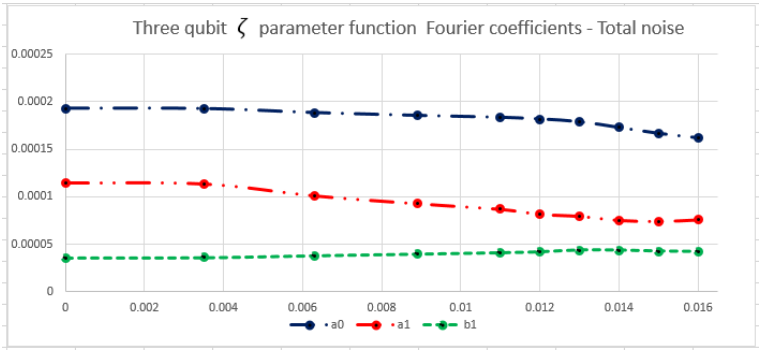

Fig. 9. Parameter function ζ Fourier coefficients as a function of total noise for the 3-qubit system. Lines are drawn to guide the eye.

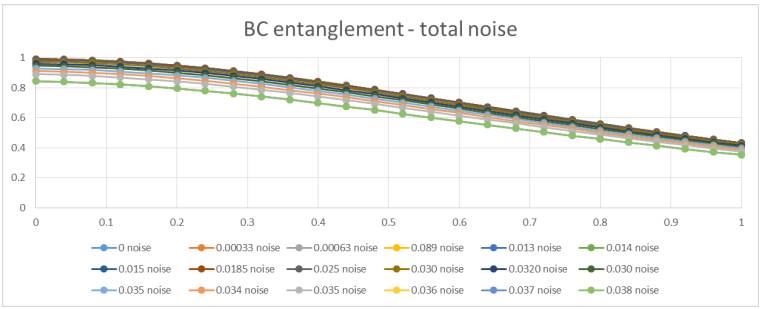

Fig. 10. Testing at different noise levels for the pure state P for a three-qubit system, as a function of γ.

We now choose an exemplar mixed state M, where

$$M = \begin{pmatrix} 0.5 & 0 & 0 & 0.5 & 0 & 0 & 0 & 0 \\ 0 & \gamma & 0 & 0 & 0 & 0 & 0 & 0 \\ 0 & 0 & 0 & 0 & 0 & 0 & 0 & 0 \\ 0.5 & 0 & 0 & 0.5 & 0 & 0 & 0 & 0 \\ 0 & 0 & 0 & 0 & 0 & 0 & 0 & 0 \\ 0 & 0 & 0 & 0 & 0 & 0 & 0 & 0 \\ 0 & 0 & 0 & 0 & 0 & 0 & 0 & 0 \\ 0 & 0 & 0 & 0 & 0 & 0 & 0 & 0 \end{pmatrix}$$

For this state we should also expect to have full pairwise entanglement for the BC pair when $\gamma = 0$, which would also decrease as γ increases. Figure 11 shows testing of M at similar noise levels. Again the entanglement indicator is relatively stable. Many similar pure and mixed states have been tested; results are uniformly good.

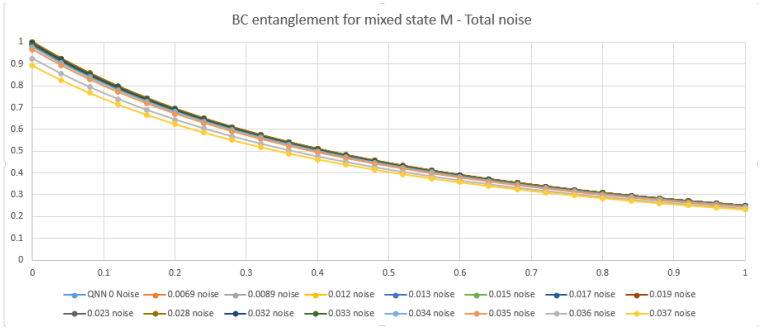

Fig. 11. Testing at different noise levels for a mixed state M, for the three-qubit system, as a function of γ.

3.2 Four and five qubit systems

The evidence of improvement in training and in testing as well as the stability to noise and decoherence in a three qubit system is clear. We will now show that the system becomes more stable as we increase the size of the system. This improvement in the results should not be surprising since the bigger the system, the more connectivity we have in our network. Note that for the larger qubit system we still use the four training states (Bell, P, Flat and C) for each pair of qubits, then, in addition, training pairs for three-way, four-way, and so on, GHZ states. See [17] for details. So, for example, for the four-qubit system, there are $\binom{4}{3} = 4$ three-way GHZ states: ABC, ABD, ACD, and BCD. Again, since this is a simulation, we can separate out noise and decoherence into two problems, and also combine them together to get 'total noise'. To demonstrate the improvement in robustness, we examine the most noise-sensitive parameter function, K. Figures 12 and 13 show the parameter functions K for the four and five qubit systems respectively.

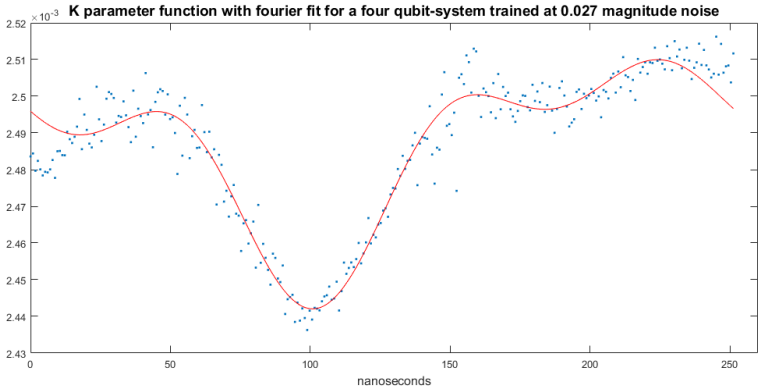

Fig. 12. Parameter function K for a 4-qubit system trained at 0.027 level of noise with its Fourier fit.

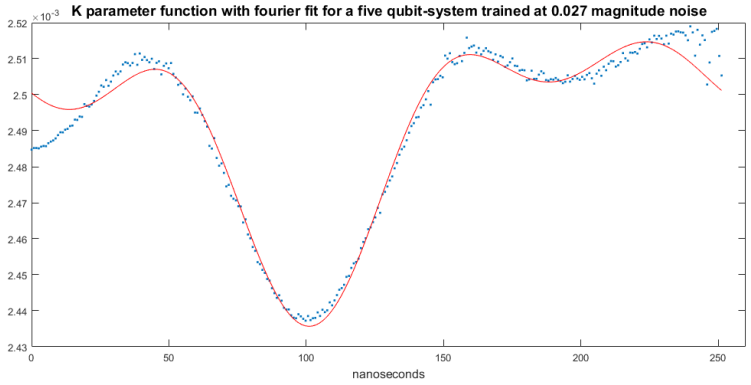

Fig. 13. Parameter function K for 5-qubit system trained at 0.027 level of noise with its Fourier fit.

Note that the noise level being added to the system in Figures 12 and 13 is almost three times as much as the noise added to the three qubit system (Figure 4); however, these results are comparable. That there is improvement in robustness is obvious. To quantify that improvement as the number of qubits increases, we plot the coefficient of determination for each of the parameter functions, R^2, as a function of the number of qubits in the system, in Figures 14-16. R^2 is defined as one minus the (normalized) sum of squares of the residuals; thus, R^2 varies from zero (bad fit) to one (perfect fit).

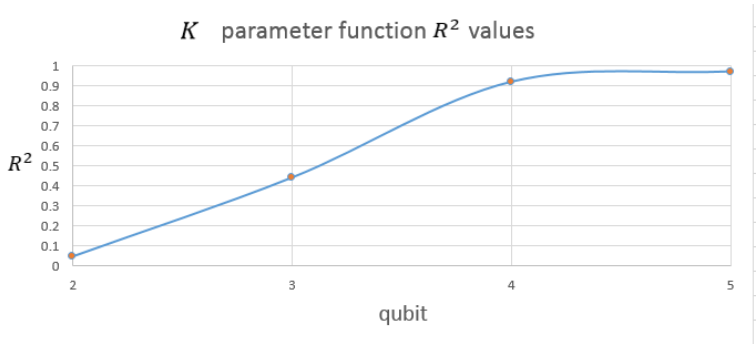

Fig. 14. R^2 as a function of number of qubits, for the K parameter function, trained at 0.02741 total noise. The line is drawn to guide the eye.

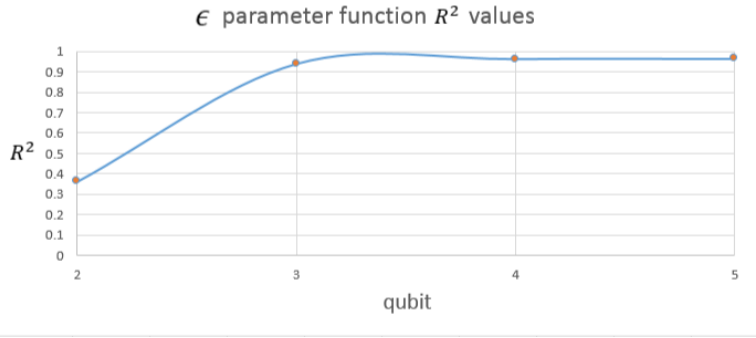

Fig. 15. R^2 as a function of number of qubits, for the ϵ parameter function, trained at 0.02741 total noise. The line is drawn to guide the eye.

As the number of qubits increases, R^2 increases towards one, and seems perhaps to approach an asymptote by four or five qubits. The increase is uniform except for the ζ parameter only (Figure 16), but even here R^2 never gets much below 0.8, and still seems to approach a high asymptote for number of qubits of four or five.

4 Learning with perturbation to the Hamiltonian

There are other ways of adding noise to the system other than perturbing the density matrix. One method is to add noise to the Hamiltonian. Of course, the system must still obey all the physical requirements to be a quantum system. A disadvantage here is we can't do decoherence

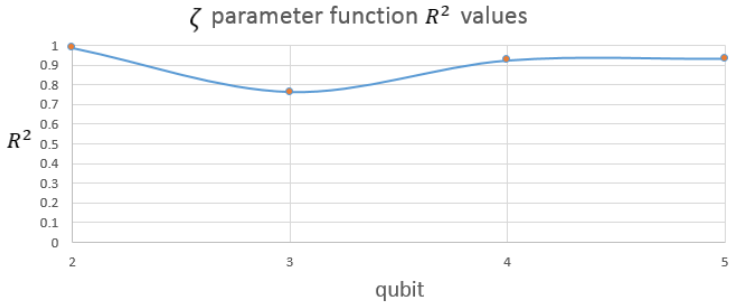

Fig. 16. R^2 as a function of number of qubits, for the ζ parameter function, trained at 0.02741 total noise. The line is drawn to guide the eye.

directly. However, our results are promising and give evidence that our system is also robust to this method of adding noise. Figures 17-20 show the ϵ parameter function trained with noise being added to the Hamiltonian for the 2-,3-,4-, and 5-qubit systems respectively.

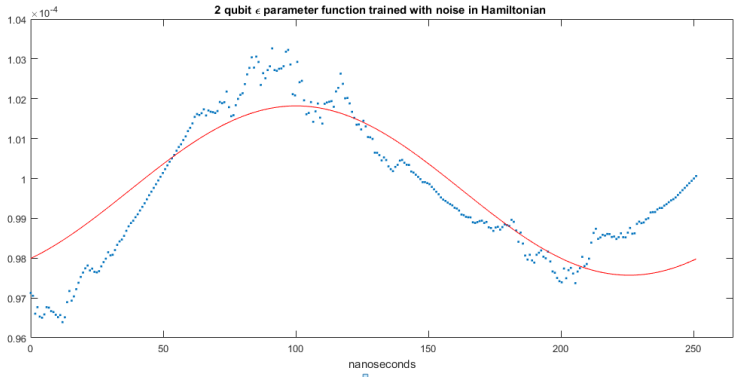

Fig. 17. Training the parameter function ϵ with noise added to the Hamiltonian instead of density matrix for a 2-qubit system

From Figures 17-20, we can see that with this alternate method of adding noise the system again becomes more stable as the number of qubits increases.

5 Discussion

The direct calculation of entanglement for a two-qubit system is relatively simple: Wootters showed[18] that the entanglement of formation could be written in closed form for a general (pure or mixed) state as

$$E_F = -\frac{1}{2}\left[1+\sqrt{1-C^2}\right]\log_2\left(\frac{1}{2}\left[1+\sqrt{1-C^2}\right]\right) - \frac{1}{2}\left[1-\sqrt{1-C^2}\right]\log_2\left(\frac{1}{2}\left[1-\sqrt{1-C^2}\right]\right) \tag{7}$$

where C is the "concurrence", defined for pure states $|\psi\rangle$ by

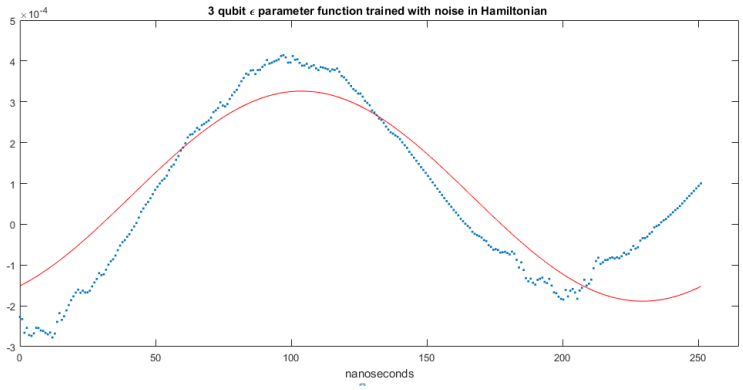

Fig. 18. Training the parameter function ϵ with noise added to the Hamiltonian instead of density matrix for a 3-qubit system

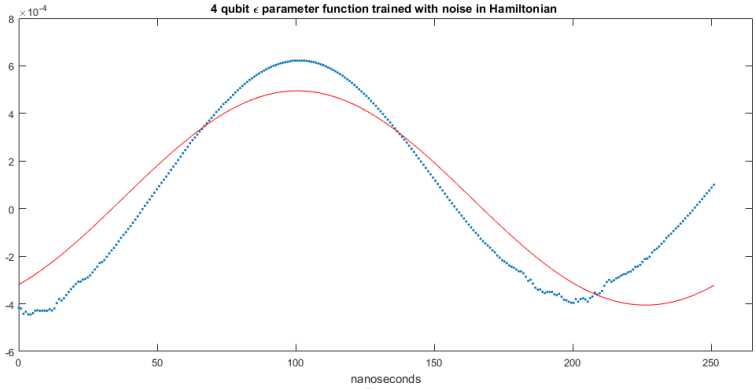

Fig. 19. Training the parameter ϵ with noise added to the Hamiltonian instead of density matrix for a 4-qubit system

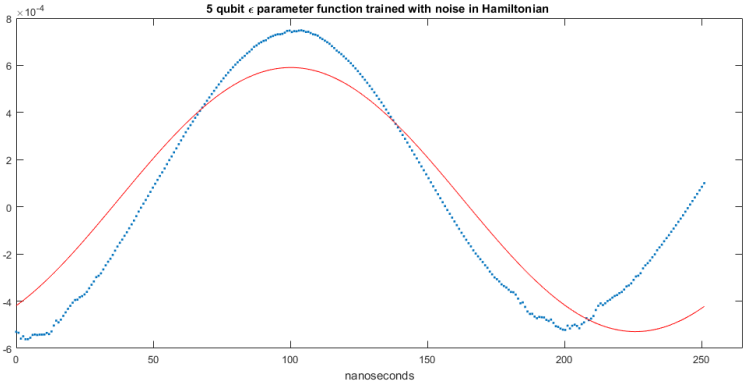

Fig. 20. Training the parameter ϵ with noise added to the Hamiltonian instead of density matrix for a 5-qubit system

$$C^2 = |\langle\psi|\psi_{sf}\rangle|^2 \tag{8}$$

where the spin flipped state $|\psi_{sf}\rangle$ is

$$|\psi_{sf}\rangle = \sigma_{yA}\sigma_{yB}|\psi^*\rangle \tag{9}$$

and the asterisk, as usual, indicates the complex conjugate. If we write (wolog) the pure state $|\psi\rangle$ as

$$|\psi\rangle = a|00\rangle + be^{i\theta_1}|01\rangle + ce^{i\theta_2}|10\rangle + de^{i\theta_3}|11\rangle \tag{10}$$

then the concurrence is given by

$$C^2 = 4[a^2d^2 + b^2c^2 - 2abcd\cos(\theta_3 - (\theta_1 + \theta_2)] \tag{11}$$

So, to estimate the entanglement of a 2-qubit pure state using our QNN, we need only to be able to estimate, or output, three measurements: $a^2d^2 + b^2c^2$, $abcd$, and $\theta_3 - (\theta_1 + \theta_2)$. (In the special case that all the coefficients are real (in this basis), we need only a single output, and the function is quadratic in the input amplitudes.) Of course, this result is also true for any pairwise entanglement of an N-qubit system. Since any admixture only diminishes the entanglement this gives us a bound for mixed states as well. For three-way entanglements of pure states we again have a closed form solution[19], which is, again, quadratic in the input amplitudes.

Now, we chose as an "output" for the QNN the average value of an experimental measure or observable O at the final time t, which (again for a pure state) has the general form

$$\langle O\rangle = \langle\psi(t)|O|\psi(t)\rangle = \langle\psi(0)|e^{iHt/\hbar}Oe^{-iHt/\hbar}|\psi(0)\rangle \tag{12}$$

For a pure product N-qubit state (the minimum flexibility in QNN training) it is easy to show that each output of this type is a sum of quadratics in the amplitudes of the input state $|\psi(0)\rangle$, with linearly independent coefficients, plus sums and products of cosines and sines in each of the phase angles in additional cross terms of the amplitudes. Because each of the parameter functions can be taken to be time varying (as we do here), this essentially means that any single output can have the complexity of almost any reasonably well-behaved function. So it is not surprising that our QNN can successfully map a smoothly varying function of a quadratic like the pairwise entanglement of formation for pure states. It is somewhat more surprising (and gratifying), that this mapping is relatively easy[15], that it generalizes well to mixed states[15, 17], that it bootstraps well to larger systems with a difficulty that decreases with size[17], and that it is robust to both noise and decoherence[13], with increasing robustness as the system gets larger (the present work). While we have no general closed form solution for N-way entanglement it is not unreasonable to think that, like pairwise and three-way, N-way is no worse than quadratic in the input amplitudes. Indeed, the fact that the QNN readily trains to find N-way entanglement provides experimental evidence that N-way entanglement is in fact no worse than quadratic. For comparison: a standard classical neural network[20] presented with the 2-qubit entanglement witness shows comparable errors on either training and testing sets only with a very much larger number of neurons (4 layers with almost a thousand neurons in total), and a comparably larger training set (1000 training pairs, versus

the four used here.) The classical neural network also does not generalize from the pure to the mixed state, as the QNN does.

There are other ways of adding noise. For example, we could suppose that the parameters in the Hamiltonian are themselves uncertain or noisy. We have checked and confirmed that this method, too, shows a similar robustness to noise. However, the disadvantage is that we can no longer can introduce decoherence. What one can do is to add noise to both the parameters (or to the Hamiltonian), and then add decoherence to the density matrix. With this procedure, again, the system is robust in both training and testing. Thus, our method seems to work up to a reasonable amount of perturbation, no matter how these perturbations are introduced. This is good for practical purposes since in reality noise and decoherence can be introduced anywhere during an experiment.

A useful quantum computer will have thousands of qubits. Based on our work so far, it seems likely that the increase in size will only improve our training and help our system to be more robust to noise and decoherence. We chose an entanglement indicator as an example problem but we would expect the same kind of effects doing other measures, for the reasons outlined above.

As the number of qubits increases, the number of epochs necessary for training each qubit goes down, but the total simulation time necessary goes up. This is to be expected since the reduction is linear but the connectivity is quadratic. Because of this our calculations were limited to a five-qubit system, but with better hardware there would be no difficulty in extending our simulations to a much larger system. Of course, once macroscopic quantum computers are available we can implement "online" training, and simulations will not be necessary.

6 Conclusions

We have successfully shown that our model of QNN calculation is robust to both noise and decoherence up to five qubits. The increased connectivity both decreases the necessary training time per qubit and increases the stability of the system, independently of the details of the noise source. This seems to be especially true for decoherence. The increased robustness is evident whether the system is trained or tested with noise. And while exact simulations like these of macroscopic quantum computers remain impractical, these results give us hope that a quantum neural approach may enable extrapolation.

Acknowledgements

We thank Mohamed Moustafa and Adrian Keister for helpful discussions, and Mohamed Moustafa for providing the NeuralWorks data.

References

1. P.W. Shor (1995), *Polynomial-Time algorithms for prime factorization and discrete logarithms on a quantum computer*, SIAM J. Comput. **26**, pp. 1484-1509.

2. S. Lloyd (2013) *The universe as quantum computer*, eprint arXiv:1312.4455.

3. G. Kalai (2009), *Quantum computers: Noise propagation and adversarial noise models* eprint: arXiv:0904.3265; G. Kalai (2011), *How quantum computer fail: Quantum codes, correlations in physical systems, and noise accumulation*, eprint: arXiv:1106.0485; G. Kalai (2016), *The quantum computer puzzle*, eprint: arXiv:1605.00992.

4. T. Albash, D.A. Lidar (2015), *Decoherence in adiabatic quantum computation*, Phys. Rev. A **91**, 062320.

5. N. Wax, (2014), *Selected papers on noise and stochastic process*, Dover.

6. A. Paetznick, B.W. Reichardt (2013), *Fault-tolerant ancilla preparation and noise threshold lower bounds for the 23-qubit Golay code*, Quantum Inf. Comput. **12**, 11-12, pp. 1034-1080

7. C.H. Bennett, D.P. DiVincenzo, J.A. Smolin, and W.K. Wootters (1996), *Mixed-state entanglement and quantum error correction*, Phys. Rev. A **54**, pp. 3824-3851.

8. Y.Glickman, S. Kotler, N. Akerman, R.Ozeri (2012), *Emergence of a measurement basis in atom-photon scattering*, Science **339**, pp. 1187-1191.

9. S. Takahasi, I.S Tupitsyn, J. van Tol, C.C Beedle, D.N Hendrickson, P.C.E Stamp (2011), *Decoherence in crystals of quantum molecular magnets*, Nature **476**, pp.7679.

10. K. Roszak, R. Filip, T. Novotny (2014), *Decoherence control by decoherence itself*, Scientific Reports 5, Article number: 9796.

11. D. Dong, M.A. Mabrok, I.R. Petersen, B. Qi, C. Chen, H. Rabitz (2015), *Sampling-based learning control for quantum systems with uncertainties*, IEEE Transactions on Control Systems Technology **23**, pp. 2155-2166.

12. A.W. Cross, G. Smith, J.A. Smolin (2015), *Quantum learning robust to noise*, Phys. Rev. A **92**, 012327.

13. E.C. Behrman, N.H. Nguyen, J.E. Steck, M. McCann (2016), *Quantum neural computation of entanglement is robust to noise and decoherence*, in Quantum Inspired Computational Intelligence: Research and Applications, S. Bhattacharyya, ed. (Morgan Kauffman, Elsevier) pp.3-33.

14. I. Aizenberg (2011), *Complex-Valued Neural Networks with Multi-Valued Neurons*, Springer.

15. E.C. Behrman, J.E. Steck, P. Kumar, and K.A. Walsh (2008), *Quantum algorithm design using dynamic learning*, Quantum Inf. Comput. **8** pp. 12-29.

16. B. Efron and R.J. Tibshirani (1994), An Introduction to the bootstrap. Boca Raton, FL: Chapman and Hall/CRC.

17. E.C. Behrman and J.E. Steck (2013), *Multiqubit entanglement of a general input state*. Quantum Inf. Comput. **13**, 1-2, pp. 36-53.

18. W.K. Wooters (1998), *Entanglement of Formation of an Arbitrary State of Two Qubits* Phys. Rev. Lett. **80**, 2245.

19. V. Coffman, J. Kundu, and W.K. Wootters (2000), *Distributed entanglement*, Phys. Rev. A **61**, 052306.

20. Neuralware (2000) *Getting started: a Tutorial in NeuralWorks Professional II/Plus*